

# Elastic, Inelastic Scatterings and Transfer Reactions for $^{16,18}\text{O}$ on $^{58}\text{Ni}$ Described by the São Paulo Potential

<sup>1</sup>J. J. S. Alves, <sup>1</sup>P. R. S. Gomes, <sup>1</sup>J. Lubian, <sup>2</sup>L. C. Chamon, <sup>1</sup>R. M. Anjos, <sup>2</sup>D. Pereira,  
<sup>2</sup>E. S. Rossi Jr., <sup>2</sup>C. P. Silva, <sup>2</sup>M. A. G. Alvarez, <sup>2</sup>G. P. A. Nobre, and <sup>3</sup>L. R. Gasques

<sup>1</sup>Instituto de Física, Universidade Federal Fluminense, Niterói, R.J., 24210-340, Brazil

<sup>2</sup>Departamento de Física Nuclear, Universidade de São Paulo,  
 Caixa Postal 66318, 05315-970, São Paulo, S.P., Brazil

<sup>3</sup>Department of Physics & The Joint Institute for Nuclear Astrophysics,  
 University of Notre Dame, Notre Dame, Indiana, 46556.

Received on 13 April, 2005

We have used a parameter - free potential, obtained from data analysis at sub-barrier energies, to explain our measurements of elastic and several inelastic scattering cross sections for the  $^{16,18}\text{O} + ^{58}\text{Ni}$  systems at an energy above the barrier. The data were analyzed through extensive coupled-channel calculations. Transfer cross sections could also be explained by the same interaction, which is consistent with the more fundamental São Paulo potential.

The imaginary part of the optical potential is the responsible for the absorption of flux from the elastic channel into any reaction mechanism. In the coupled channel formalism, if all relevant peripheral reaction channels are included in the calculations, the imaginary part of the optical potential must be assumed as negligible in the surface region. Within this context, the real part of the interaction can be unambiguously determined, as long as the elastic scattering and all important peripheral processes are measured. Previously [1, 2], we have performed such measurements for the  $^{16,18}\text{O} + ^{58,60,62,64}\text{Ni}$  systems, at the sub-barrier energy region ( $E_{Lab} \leq 38$  MeV), and the corresponding bare potentials were extracted from coupled-channel data analysis. A good test of consistency of the extracted potential would be to use it on data analysis, without any further free parameter, in the difficult energy region slightly above the Coulomb barrier, since at this region there are several open channels with strong couplings among them.

In the present paper, we show the results of the measurements and of the coupled channel (CC) calculations for the elastic scattering, seven inelastic scattering angular distributions, and three transfer reaction channels cross sections for the  $^{16,18}\text{O} + ^{58}\text{Ni}$  systems, at  $E_{Lab} \leq 46$  MeV ( $V_B \cong 40.6$  MeV).

The CC calculations were performed using the FRESKO code [3]. We have adopted a similar procedure as the one used in the sub-barrier data analysis [1, 2], by assuming a Woods-Saxon shape for the optical potential, with an inner imaginary part which takes into account the internal absorption from barrier penetration (essentially the fusion process). Previously (at sub-barrier energy regime), a large number of channels were involved in the CC calculations. No significant extra surface absorption is expected above the barrier at 46 MeV, allowing us to assume the same parameters for the volume imaginary part of the potential as before:  $W_o = 50$  MeV,  $r_{io} = 1.06$  fm, and  $a_i = 0.2$  fm. For the real part of the interaction, a Woods-Saxon set of parameters, equivalent to the São Paulo potential [4, 6] at the surface region, was assumed:  $r_{co}=r_o = 1.06$  fm,  $V_o = 273$  MeV ( $^{16}\text{O}$ ) and 113 MeV ( $^{18}\text{O}$ ),  $a = 0.59$  fm ( $^{16}\text{O}$ ) and 0.77 fm ( $^{18}\text{O}$ ).

The new measurements were performed at the São Paulo

8UD Pelletron Accelerator. We have used two different detecting systems: (i)- a set of three telescopes E- $\Delta$ E, each one consisting of one proportional counter that provides signals of energy loss ( $\Delta E$ ) in the gas, and of the remaining energy (E) detected in a surface barrier detector, and (ii)- a set of nine surface barrier detectors. For both detection sets, the angle determination was made by reading on a goniometer with a precision of 0.5°. Each spectrum was accumulated during five continuous days, in order to obtain statistics good enough to identify very small cross sections.

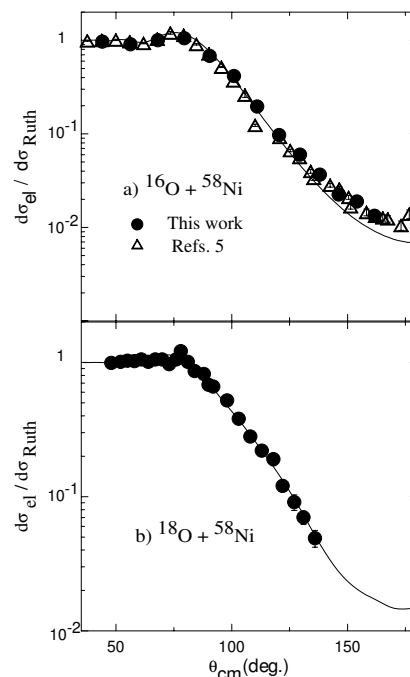


FIG. 1: Elastic scattering angular distributions for the  $^{16}\text{O} + ^{58}\text{Ni}$  and  $^{18}\text{O} + ^{58}\text{Ni}$  systems. The curves are the results from coupled channel calculations, without any free parameter.

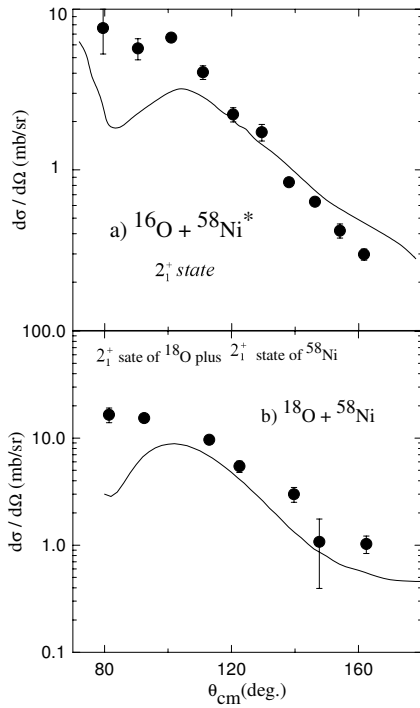


FIG. 2: Inelastic scattering angular distributions for the (a)  $2_1^+$   $^{58}\text{Ni}$  excited state in the  $^{16}\text{O}$  scattering, (b) sum of the  $2_1^+$   $^{58}\text{Ni}$  and  $2_1^+$   $^{18}\text{O}$  excited states in the  $^{18}\text{O}$  scattering. The curves are the parameter - free coupled channel calculations.

We were able to identify the elastic scattering, inelastic scatterings to the first  $2_1^+$  excited state of the  $^{58}\text{Ni}$ , the two-phonon excitations of the triplet  $2_2^+$ ,  $0_2^+$  and  $4_1^+$  states of the  $^{58}\text{Ni}$ , the  $2_1^+$  state of the  $^{18}\text{O}$ , alpha stripping transfer for the  $^{16}\text{O} + ^{58}\text{Ni}$  system and one and two neutron stripping transfer channels for the  $^{18}\text{O} + ^{58}\text{Ni}$  system. The data are shown in figures (1-4) – (a) for the  $^{16}\text{O} + ^{58}\text{Ni}$  system and b) for the  $^{18}\text{O} + ^{58}\text{Ni}$ . For one-neutron transfer channel, the data include transitions to the ground state, the first  $^{17}\text{O}$  excited state, and four  $^{59}\text{Ni}$  excited states. For two-neutron transfer channel, the data include transitions to the set of states with excitation energy from 0 to 6.5 MeV, including 23 excited states of  $^{60}\text{Ni}$  and the two first excited states of the  $^{16}\text{O}$  [4]. For alpha transfer, the data include transitions to the ground states of  $^{62}\text{Zn}$  and  $^{12}\text{C}$ , several excited states of  $^{62}\text{Zn}$  and the 4.4 MeV excited state of  $^{12}\text{C}$ . The experimental resolution was not good enough to precisely separate the inelastic excitations to the  $2_1^+$  states of  $^{18}\text{O}$  and  $^{58}\text{Ni}$  and, therefore, the corresponding data refers to the contribution of both states. Also, the two-phonon triplet states are summed together.

In the CC calculations, the inelastic couplings were treated within the vibrational mode, with the same deformation lengths assumed in the sub-barrier data analysis. A one-step cluster transfer of one  $s=0$  neutron pair was assumed for the two-neutron transfer process. Due to the large number of states for neutron transfer, most of them with unknown spectroscopic factor, we have adopted an average value for all states

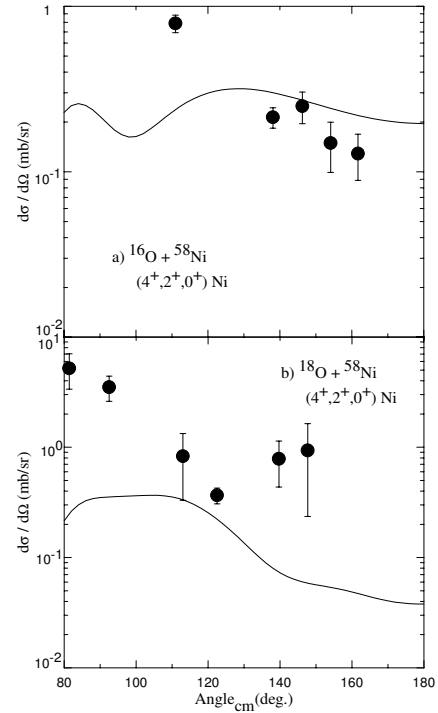


FIG. 3: Two-phonon inelastic scattering angular distributions for the  $0_2^+$ ,  $2_2^+$  and  $4_1^+$   $^{58}\text{Ni}$  excited states by the interaction with (a)  $^{16}\text{O}$ , (b)  $^{18}\text{O}$  projectiles. The curves are the results from coupled channel calculations, without any free parameter.

equal to 0.87, which was used at the sub-barrier study. For alpha transfer in the  $^{16}\text{O} + ^{58}\text{Ni}$  system, we also included some states with unknown spectroscopic factors. As there were no available spectroscopic factor values from the sub-barrier energy studies, these were the only free parameters in our present calculations. The average value of 1.26 was used for all these states.

The results for the cross sections obtained from CC calculations are shown in figures (1-4). The predictions are in reasonable agreement with the data, except in three situations, always at forward angles. The first is for the inelastic excitation of the  $^{58}\text{Ni}$  triplet for both systems. In this case, however, the discrepancy may be connected with some contamination of the inelastic scattering data with the low energy tail of the elastic peak, which is intense at forward angles. In the backward region the elastic peak presented a much less pronounced tail. The other situations are for the alpha and two-neutron transfer processes at forward angles, where average spectroscopic factors were adopted. The two - neutron transfer has very small cross sections, and at the forward angles it was difficult to separate it from the more intensive one-neutron transfer channel. Concerning the alpha - transfer, the highest excited states could be contaminated, at forward angles, by the 4.4 MeV inelastic excitation of  $^{12}\text{C}$  target contamination. In the elastic scattering data for the  $^{16}\text{O} + ^{58}\text{Ni}$  system, we have also included some data available in the literature[5].

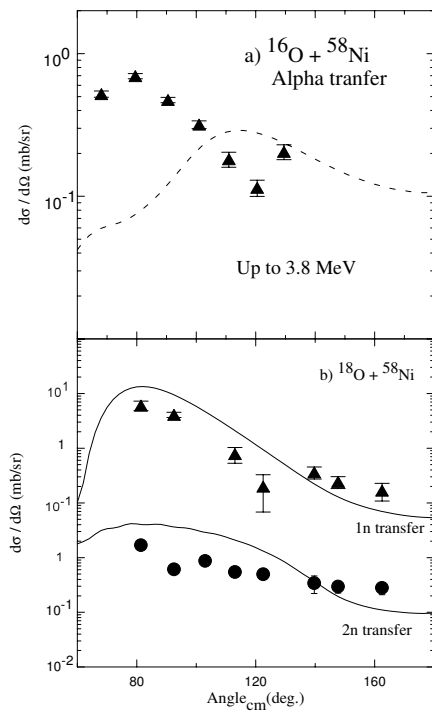


FIG. 4: Transfer channel differential cross sections. (a) Alpha stripping channel in the  $^{16}\text{O} + ^{58}\text{Ni}$  system. (b) One-neutron and two-neutron channels in the  $^{18}\text{O} + ^{58}\text{Ni}$  system. The curves are the results from coupled channel calculations, with only one free parameter, the average spectroscopic factor for alpha transfer in  $^{16}\text{O} + ^{58}\text{Ni}$ .

In summary, we have obtained experimental differential cross sections of several peripheral reaction channels for the  $^{16,18}\text{O} + ^{58}\text{Ni}$  systems at  $E_{\text{Lab}} = 46$  MeV. The data have been analyzed within extensive coupled-channel calculations and using the same interaction that had been obtained in previous analysis of sub-barrier data. Only one free parameter was included in the calculations, the average spectroscopic factor for alpha transfer of the  $^{16}\text{O} + ^{58}\text{Ni}$  system. A reasonable agreement between data and theoretical predictions was obtained. Therefore, we have demonstrated the consistency of the simultaneous data analysis, from the sub-barrier region to energies above the barrier, with the same potential. We point out that the Woods-Saxon optical potentials assumed in this work are also consistent[2] with the more fundamental São Paulo interaction that is based on the folding potential and on the effects of the Pauli non-locality.

### Acknowledgments

This work was partially supported by Financiadora de Estudos e Projetos (FINEP), Fundação de Amparo à Pesquisa do Estado do Rio de Janeiro (FAPERJ), Fundação de Amparo à Pesquisa do Estado de São Paulo (FAPESP), Conselho Nacional de Desenvolvimento Científico e Tecnológico (CNPq), CAPES, and The Joint Institute for Nuclear Astrophysics (JINA) NSF PHY 0216783.

- [1] L. C. Chamon et al, Nuclear Physics A **597**, 253 (1996).  
 [2] E. S. Rossi Jr. et al, Nuclear Physics A **707**, 325 (2002).  
 [3] I. J. Thompson, Computer Physics Report **7**, 167 (1988).  
 [4] L. C. Chamon et al, Physical Review C **66**, 014610 (2002).

- [5] Leon West Jr., K. W. Kemper, and N. R. Fletcher, Physical Review C **11**, 859 (1975).  
 [6] J. J. S. Alves et al, Nuclear Physics A **748**, 59 (2005).